Chemical Probe-based Nanopore Sequencing to Selectively Assess the RNA Modifications

Soundhar Ramasamy[1†], Vinodh J. Sahayasheela[2†], Surbhi Sharma[1], Zutao Yu [1], Takuya Hidaka[1], Li Cai[3], Vaijayanthi Thangavel[1], Hiroshi Sugiyama[1,2*], Ganesh N. Pandian[1*]

[1] Institute for Integrated Cell-Material Science (WPI-iCeMS), Kyoto University, Sakyo Ku, Kyoto 606-8501, Japan.

[2] Department of Chemistry, Graduate School of Science, Kyoto University, Sakyo Ku, Kyoto 606-8502, Japan.

[3] Cell and Developmental Biology Graduate Program, Department of Biomedical Engineering, Rutgers University, Piscataway, NJ 08855, United States of America.

[†]Both authors contributed equally to the work

Corresponding author email - namasivayam.ganeshpandian.5z@kyoto-u.ac.jp**,** hs@kuchem.kyoto-u.ac.jp

ABSTRACT: Nanopore direct RNA sequencing (dRNA-Seq) reads reveal RNA modifications through consistent error profiles specific to a modified nucleobase. However, a null dataset is required to identify actual RNA modification-associated errors for distinguishing it from confounding high intrinsic sequencing errors. Here, we reveal that inosine creates signature mismatch error in dRNA-Seq reads and obviates the need for a null dataset by harnessing the selective reactivity of acrylonitrile for validating the presence of actual inosine modifications. Selective reactivity of acrylonitrile towards inosine altered multiple dRNA-Seq parameters like insertion frequency, signal intensity and trace value. We also deduced the stoichiometry of inosine modification through deviation in signal intensity and trace value using this chemical biology approach. Furthermore, we devised Nano ICE-Seq, a protocol to overcome the low coverage issue associated with direct RNA sequencing. Taken together, our chemical probe-based approach may facilitate the knockout-free detection of disease-associated RNA modifications in clinical scenarios.

KEYWORDS: Chemical probe • Direct RNA sequencing • Nano ICE-Seq• RNA modifications • Selective reactivity

A total of 172 RNA modifications[1] collectively termed "Epitranscriptome" are known to exist in biological systems. RNA Modifications exert a spectrum of regulatory function over cellular RNAs ranging from base pairing to protein binding[2]. Adenosine- to-inosine (A-I) is one of the highly abundant post-transcriptional RNA modifications catalyzed by adenosine deaminase. These modifications regulate neuronal response, ion channel conformations, and neural signaling in the brain[3]. At the RNA level, A-I editing alters coding potential[4],[5], stability[6], decay[7], translation[4], and microRNA binding[8]. Accordingly, dysregulation of A-I editing enzymes and their co-regulatory proteins are implicated in complex diseases from cancer to neurological disorders[9]. Consequently, differential A-I editing landscape can potentially serve as disease-specific diagnostic biomarkers. However, the method to rapidly profile them in a clinical scenario is still underexplored. Most RNA modification profiling methods use sequencing by synthesis (SBS) chemistry that requires reverse transcription (RT) of RNA into DNA. While most RNA modifications are RT-silent, A-I editing shows A > G or U>C mutation profiles and is a reliable proxy for A-I calling. Paired genome sequencing[10] (or) ADAR knockout transcriptome [11] (or) acrylonitrile-based chemical erasing of inosine reads[12] are some of the methods employed for high confident detection of A-I editing sites. Though the acrylonitrile-based approach is easy to adapt, it carries over the limitation of the SBS platform, such as a) laborious sample preparation, b) lesser reproducibility due to multi-step sample/library preparation, c) error-prone stoichiometry estimates caused by RNA fragmentation and d) difficulty to simultaneously map multiple modifications in a single run[13]. Branton D, Deamer DW, and Bayley H et al. first demonstrated direct RNA/DNA sequencing of synthetic oligonucleotides using *S. aureus* α-hemolysin pore[14,15]. Turner and colleagues also demonstrated direct sequencing of RNA using *E. coli* curli transport channel CsgG pore[16].

Oxford Nanopore Technology (ONT) operates by ratcheting DNA/RNA into the modified version of this dual constricted CsgG pore. The migrating nucleic acid triggers a distinct change in the stable current maintained across the pore. The resulting pattern is base called to a corresponding nucleic acid sequence with machine learning algorithms. dRNA-Seq obviates the need for reverse transcription and overcomes the need for laborious protocols used in SBS platforms. Furthermore, dRNA-Seq uses the native RNA, their current pattern and mapped reads reveal RNA modifications primarily as mismatch errors or as a change in other parameters[17,18,19,20]. Above ONT parameters associated with RNA, modifications are readily available from dRNA-seq reads without any chemical/antibody treatment on native RNA.

In this work, we focused on A-I editing sites detection from dRNA-Seq reads. We employed a long synthetic transcript harboring identical K-mers as that of biologically occurring A-I editing sites and identified mismatch error as an accurate predictor of A-I modification. However, the RNA modification associated errors in dRNA-Seq reads are

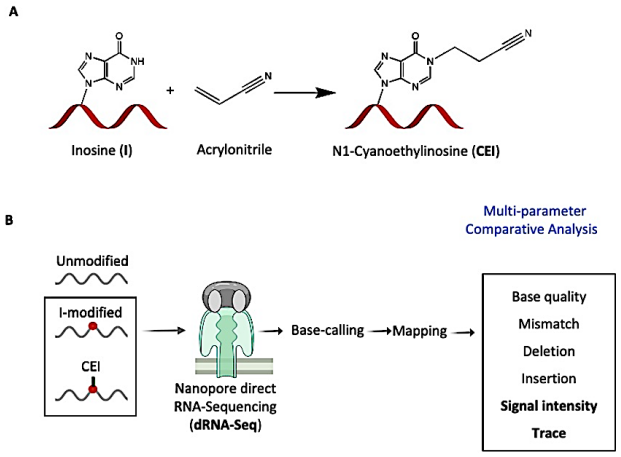

Figure 1. Schematics of acrylonitrile cyanoethylation reaction and overview of the workflow. (A) Acrylonitrile selectively reacts with Inosine (I) to give N1-cyanooethylinsoine (CEI) (B) Overview of the workflow used in this study to identify I-modification using acrylonitrile reactivity from direct RNA-Seq reads.

also confounded by single-nucleotide polymorphism/variations (SNP/SNV) or the intrinsic ONT platform noise. Accordingly, Liu et al. devised a strategy to identify N6-methyladenosine RNA modification-associated mismatch errors by comparing the wild-type RNA with modifications and contrasting them with the modification-free RNA derived from the knockout studies[21]. For validating inosine(I)-modification associated mismatch error, we harnessed the selective reactivity of acrylonitrile with inosine to induce measurable deviations over dRNA-Seq parameters (**Figure 1**). We also show acrylonitrile-induced deviations were adequate to validate the presence of actual I- modification in our RNA models in a knock-out independent manner.

Inosine modification associated mismatch error accurately reveals A-I modification from dRNA-Seq reads

In ONT-Direct RNA Sequencing (dRNA-Seq) platform, the reads are defined through multiple parameters such as current intensity, trace, dwell time, base quality, mismatch errors, deletion, and insertion. The presence of RNA modification is shown to alter one or more of the above parameters in a modification-specific manner. To systematically evaluate which of the above dRNA-Seq parameter is perturbed by the presence of A-I modification, we devised a workflow (**Figure S1**) and synthesized short and long RNA transcripts containing inosine harboring identical K-mers as that of biologically occurring A-I editing sites (approximately 50 % incorporation, see methods for details, **Figure S2**). The dRNA-Seq of unmodified (UM) and inosine(I) modified transcripts have shown consistent mismatch error on I-modified sites when compared to unmodified sites **(Figure 2A & B)**. To comparatively identify the key parameter contributing to differentiate UM from I-modified transcripts, we extracted four parameters (base quality, mismatch, insertion, and deletion) from all possible 5-mers (-2, -1, 0, 1, and 2). Since the gradual migration of 5-mer inside the pore is measured as "squiggles," we employed 5-mer related parameters for all our downstream analysis[21].

Principal component analysis (PCA) on K-mers from UM and I-modified with four parameters forms distinct clusters. The control K-mers derived from UM and I-modified transcripts fail to form distinct clusters. This indicates that the changes in dRNA-Seq parameters are I-modification specific (**Figure 2C, Figure S3**). We then generated a support vector machine and applied it independently on all parameters (see the methods) to statistically rank the parameter's ability in distinguishing UM from I-modified K-mers. Among the four tested parameters, mismatch error was shown to predict the modification with high accuracy (> 80 %). On the other hand, SVM on control K-mers lacked accurate prediction on modified K-mers (**Figure 2D**). Importantly, the differentiating capability of mismatch error could be reproduced across independent replicates. Thus, the

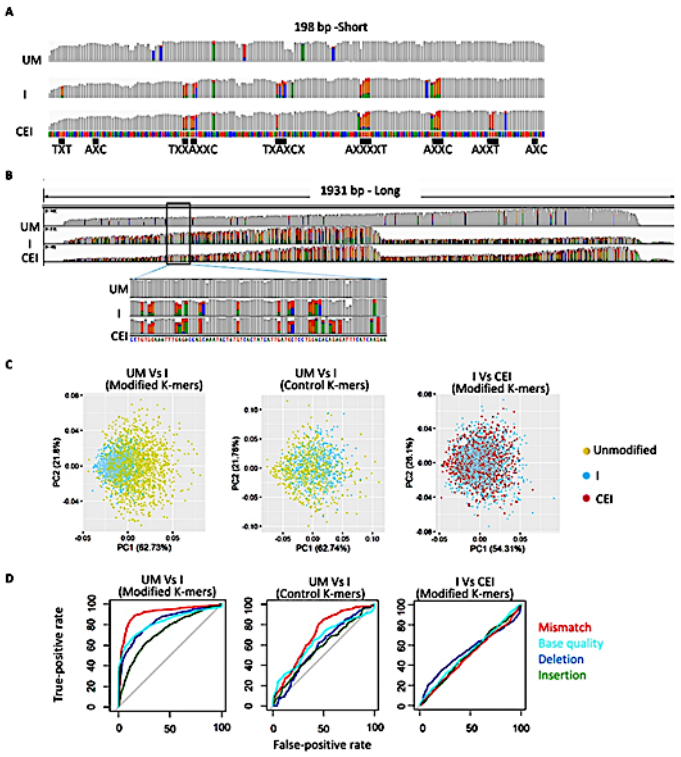

Figure 2. Mismatch error act as an accurate proxy for inosine identification from dRNA-Seq reads. (A&B) IGV snapshots of short (A) and long IVT transcripts (B) used in this work. unmodified –UM(G), Inosine modified 50%- I and cyanoethylation treatment- CEI transcripts showing mismatch errors. Mismatch frequency > 0.1 are represented in color. Green(adenosine), orange (guanosine), blue (cytosine) and red (thymine). Bold underline and the accompanying sequence represent the pre-determined sites of inosine (X) incorporation during IVT synthesis (C) Principal component analysis (PCA) plot showing the first two principal components. Each dot represents a five-nucleotide K-mer in the synthetic sequence and has been colored based on the condition. The PCA is performed using 15 features (Mismatch, insertion, deletion, and base quality) extracted across five positions (-2, -1, 0, 1, 2) from each K-mers. Modified K-mers contain a minimum of one pre-determined modification site, while control K-mer is derived from other regions of the transcript. Colors represent K-mers transcripts identity as UM (yellow), I (blue), and CEI (maroon). (D) ROC curve showing SVM prediction power using features- mismatch (red), insertion(green), deletion (blue) and base quality (cyan) on separating K-mers derived from UM, I and CEI transcripts.

results substantiate the reliability of I-modification associated mismatch errors in predicting A-I editing sites from dRNA-Seq reads.

To comparatively analyze the signal intensity parameter, we employed TOMBO22 packages to statistically score significant signal difference (Δ signal difference) between UM and I-modified IVT RNA (short). The first step in the TOMBO workflow is `resquiggle`, where the raw signal is matched to the corresponding sequence. The second step is to perform comparative analysis using raw signals to identify regions with Δ signal difference. TOMBO uses the Kolmogorov–Smirnov test (K-S test) to calculate Δ signal differences with a score ranging from zero to one where the values moving towards one indicate the regions with a maximal signal difference. TOMBO computed statistics only for selected regions in the long-modified transcripts (data not shown). Therefore, only the short I-modified were used for all TOMBO analysis and it showed calculations evenly across its length. Comparison of UM and I-modified transcripts signals showed that the Δ signal differences were mostly around I-modified sites. All the I-modified sites were captured by TOMBO calling for sequences with Δ signal difference, but they also captured a few unmodified sites **(FigureS4)**. Though TOMBO shows Δ signal differences between UM and I-modified transcripts, it is still not a reliable parameter for A-I sites identification owing to the dispersal of signal differences peak from actual I-modified sites. Therefore, mismatch errors serve as a more accurate proxy to detect I-modification with single-base resolution from dRNA-Seq reads.

Acrylonitrile reactivity validates inosine-associated mismatch error by altering the current signal

To verify if inosine modifications associated mismatch error (MAME) can be validated through chemical adducts, we explored if we can adapt the acrylonitrile selective reactivity (**Figure 1**) towards I-modification in the dRNA-Seq platform. Acrylonitrile selectively cyanoethylate I-modification at N1 position to form N1-cyanoethyl inosine (CEI)[23] (**Figure 1A**). CEI transcripts were generated by treating the I-modified transcripts (short) with acrylonitrile. Initially, acrylonitrile treatment was performed on transcript where all predetermined sites in synthesized RNA molecules contain I-modification (100% inosine). But this fully modified transcript after acrylonitrile treatment yielded failed reads (q score < 7) during dRNA-Seq runs. On the contrary, our in vitro transcribed (IVT) RNA with approximately 50% of inosine incorporation yielded usable (pass) reads after acrylonitrile treatment. Therefore, we used the I-modified transcripts for cyanoethylation reaction. RNA was treated with acrylonitrile for 30 mins [23,] and the reactivity was confirmed using HPLC and mass spectrometry (**Figure S2)**. The size and concentration of RNAs were confirmed using a bioanalyzer (**Figure S5A)**. Our APCA and SVM analysis from 5-mers derived from I and CEI transcripts revealed that none of the four parameters i.e., base quality, mismatch, insertion, and deletion, could be used for classification and ensuing prediction **(Figure 2C)**.

On the other hand, TOMBO analysis based on Δ signal difference efficiently captured all I-modified sites, whereas they also captured a few unmodified sites **(Figure 3A-F and Figure S4B)** as observed in the UM *vs.* I-modified condition. But it is important to note here that in the chemical probe-based condition, the dispersal of the signal difference can be corrected using I-MAMEs. Therefore, MAMEs act as the proxy for I-modification base resolution and Δ signal differences could be used for validation. It is also important to note here that all our results were derived from transcripts with 50% I-modification, but under *in vivo* conditions, the overall A-I editing levels were shown to range from 77% to

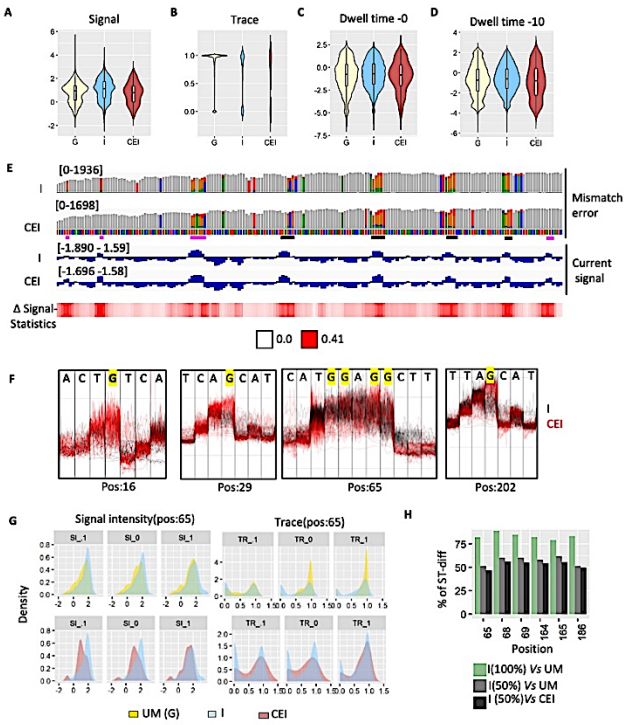

Figure 3. Chemical probe-based dRNA-Seq validates inosine sites using signal and trace value difference. Violin plot showing kernel density estimate & inner boxplot showing interquartile range and median of unmodified (UM)-G, inosine modified-I and acrylonitrile treated inosine (CEI) nucleobase. (A)signal (B) base probability (trace), (C) dwell time of RNA in the center of the CsgG pore (Dwell Time-0) and (D) that in the center of ATP-dependent motor protein helicase (Dwell Time-10) (E) IGV snapshot showing mismatch error profile and TOMBO based signal comparison between I (50%) and CEI (50%) transcripts. The K-S test was used to compute signal difference (Δ signal) statistics between I and CEI conditions. The sites with K-S test value > 0.2 are considered to harbor statistically significant signal difference. Mismatch frequency > 0.05 are represented in color. Green (adenosine), orange (guanosine), blue (cytosine) and red (thymine). (F) TOMBO raw signal overlay plot for selected regions between I and CEI transcripts. The nucleotide highlighted in yellow are pre-determined inosine incorporation sites. (G) Density plot showing distribution of signal intensity (SI) and trace (TR) among unmodified-G, modified-I and CEI conditions. The distributions are shown for position 65 in the synthetic RNA (position '0' in the figure) and its upstream and downstream positions as -1 and +1 (see above, Figure 3F). (H) Grouped bar plot showing signal and trace value difference (ST-diff) by comparing I-modified sites in I-100%, I-50% and CEI conditions using nanoRMS- KNN classification algorithms. The signal intensity and trace from -1, 0, +1 sites were used for the calculation.

1.2 % in human tissues[24]. Accordingly, we computationally estimated the effect of inosine concentration in the acrylonitrile-based validation method by gradually reducing the modified reads in I-modified and CEI conditions with unmodified reads. The results showed that the minimal concentration detected by our chemical probe-based dRNA-Seq approach is about 40% **(Figure S6)**. Therefore, dRNA-Seq approach is more suitable for recovering the heavy or moderate A-I editing sites. Further improvements like the targeted approach to be detailed in the following section could overcome this detection limit.

Acrylonitrile alters the trace value of inosine modified sites

TOMBO comparative analysis considers only the signal difference. However, along with the signal difference, the base probability (trace), dwell time of RNA in the center of the CsgG pore (Dwell Time-0, DT-0), and that in the center of ATP-dependent motor protein helicase (Dwell Time -10, DT-10)[18] were also observed to be altered (**Figure 3A**). Recently Begik et al. developed a workflow termed nanoRMS, where RNA modification was shown to deviate both signal and trace values of dRNA-Seq reads. Hence, we followed the nanoRMS workflow to collectively measure the signal and trace value difference (ST-diff) induced by I-modification and CEI. (Note: nanoRMS estimates stoichiometry, considering acrylonitrile reactivity is not quantitative, we refer to it as ST-diff). We first estimated the ST-diff induced by I-modification by comparing the modified sites in 100% and 50% I-modified K-mers against UM transcript. The 100% I-modified transcript showed ST-diff in the range of 79%-89%. On the other hand, for the 50% I-modified transcript, we observed the expected decrease in ST-diff, 51%-61%. In the case of CEI, ST-diff was 49-56%. Thus, the nanoRMS quantification clearly shows that CEI adducts could significantly perturb the signal and trace value of dRNA-Seq reads as inosine modification. Taken together, it is evident that CEI creates a significant change in signal and trace value.

Chemical probe-based dRNA-Seq assess pseudouridine sites

Acrylonitrile also reacts with pseudouridine (Ψ) to form N1- cyanoethyl Ψ (CEΨ); however, the reactivity is much lower when compared to that with I-modification[23] in our followed reaction condition **(Figure S7)**. Also, CEΨ cannot stall reverse transcriptase during cDNA synthesis and remains silent and undetectable in the SBS platform[25]. Hence, we explored whether acrylonitrile reactivity towards Ψ can reveal actual Ψ sites in dRNA-Seq reads by following a similar workflow described for I modification. As shown in **Figure S8**, we observed Ψ associated mismatch errors where Ψ has been misinterpreted as either C or U nucleobase, while similar observations were reported by [19],[26],[20],[18]. PCA on K-mers further revealed that the two parameters (base quality and mismatch errors) could sort K-mers into UM and Ψ modified clusters **(Figure S8G and S8H)**. Like CEI adduct, CEΨ not altered parameters like base quality, mismatch, deletion, and insertion, but shows Δ signal differences in TOMBO comparative analysis between Ψ and CEΨ showed around actual Ψ modification sites **(Figure S9)**. Since the reactivity of acrylonitrile towards Ψ modification is partial under our followed reaction condition, we have not further explored Ψ modification in our work. But we should also be aware that acrylonitrile shows mild cross-reactivity with modifications other than I and Ψ [27]. Still, those modifications are less abundant and not explored in this study.

Targeted approach reveals in vivo transcriptome A-I editing sites

We then tested our chemical probe-based dRNA-Seq method on mouse brain poly-A enriched mRNA. We generated the CE (-) mock-treated datasets, in which RNA is subjected to 70 °C for 30 min without acrylonitrile, and acrylonitrile-treated referred to as CE (++) **(Figure 3A and S1B)**. The acrylonitrile reactivity on the mouse transcriptome was confirmed using cyanoethylation coupled with Sanger sequencing, a gold standard method for A-I validation. As expected, we observed cyanoethylation-mediated 'G' peak depletion in the bonafide A-I editing sites on Gria2, Kcan1 gene (**Figure S10**)[25]. All the samples were sequenced using independent flow cells, the resulting FAST5 files were base called to FASTQ files using GUPPY and mapped using Minimap2 against the mouse transcriptome references (refer methods). The gene count shows a good correlation within biological replicates (r=0.93 & 0.95)

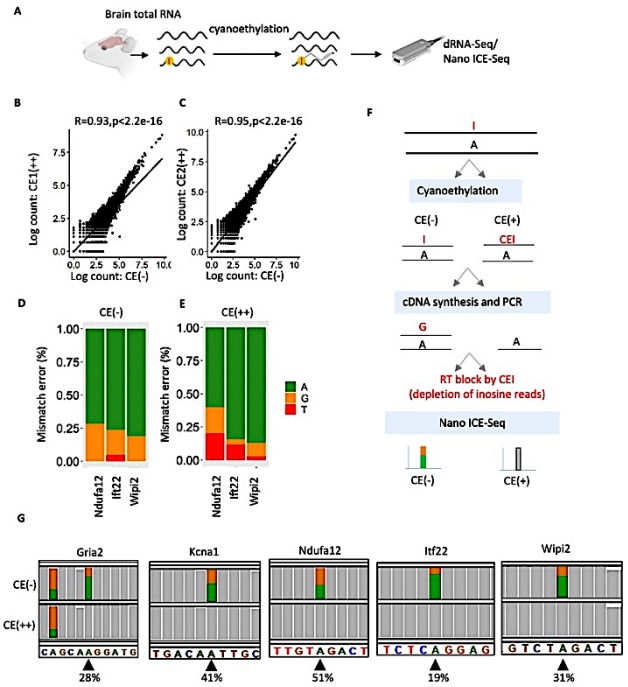

Figure 4. Targeted approach reveals in vivo transcriptome A-I editing sites (A) Overview showing different conditions of mouse brain samples subjected to nanopore sequencing. (B&C) Agreement between different conditions of mouse brain dRNAseq (B) CE (-) versus CE1(++) and (C) CE (-) versus CE2(++). (D&E) Barplot showing mismatch frequency on pre-annotated inosine modification sites from dRNA-Seq run. (D) CE (-) and (E) merged reads from biological replicates CE (++). (F) Schematics depicting Nano ICE-Seq workflow (G) IGV snapshot of CE (-) versus CE2(++) showing depletion of guanosine upon cyanoethylation in Gria2, Kcna1, Ndufa12, Itf22, Wipi2 in mouse brain. Mismatch frequency > 0.2 are represented in colours. Green(adenosine), orange (guanosine), blue (cytosine) and red (thymine).

and an independently published mouse brain dRNA-Seq transcriptome (r=0.84-0.87) **Figure 4B, Figure S11**. Mapping statistics, N50 revealed moderate fragmentation of input RNA due to the high temperature used in acrylonitrile treatment **(Table S1)**. Due to the low coverage of our dRNA-Seq datasets **(Table S1)**, we chose to evaluate the previously reported A-I and Ψ sites from RADAR[28], REDI portal database[29] and published literature[30]. We filtered bonafide sites overlaps with the SNP database (dSNP 142) **(Figure S1B)**. We chose to have a read count cut-off (> 5 reads) that yielded thirteen and twenty-seven bonafide A-I and Ψ sites with mismatch errors **(Table S2 and S3)**. As shown in the representative genes (**Figure 4D and 4E**), the *in vivo* A-I editing sites captured using dRNA-Seq showed I-associated mismatch errors. Considering the biological relevance of four genes (Ndufa12, Wipi2, Tox4, and Itf22) implicated in social stress and neuropsychiatric disorders, we performed cyanoethylation-based Sanger validation of four A-I editing sites (**Figure 4F-H**). The Sanger validation revealed that the dRNA-Seq mismatch error inferred as the I in the Tox4 site harbored SNV **(Figure S12)**.

We also developed a workflow termed `Nano ICE-Seq` for targeted validation of I sites by combining the chemical probe with ONT cDNA-Sequencing **(Figure 4F)**. We performed multiplexed PCR for amplifying selected inosine sites (Gria2, Kcna1, Ndufa12, Wipi2, and Ift22) from mouse brain RNA subjected to CE (-) and CE (++) conditions. Interestingly, Nano ICE-Seq efficiently recovered the bonafide A-I sites in Gria2 and Kcna in the mouse brain that were not captured in our mouse brain dRNA-Seq[25]. In general, the I-modified site in RNA gets converted to "G" upon reverse transcription. These "G" disguised I-modified reads are further depleted in acrylonitrile conditions due to the stalling of reverse transcriptase by CEI adduct. Accordingly, in Nano ICE-Seq, the CE (++) condition shows depletion of "G" on all the tested A-I editing sites **(Figure 4G)**. Nano ICE-Seq workflow is beneficial when low coverage is an issue. Furthermore, Nano ICE-Seq's total workflow from experiment to analysis ranges 24-30h, and it can be adapted in clinical scenarios for A-I editing screens with diagnostic potential.

Discussion

Recently, RNA modification-associated mismatch errors (MAMEs) have been used as a proxy for profiling modification from dRNA-Seq reads. Here, we have shown that A-I editing can be accurately identified using mismatch error with an accuracy greater than 80% using synthetic RNA and support vector machine learning (**Figure 2**). However, there is a need for comparative analysis using an unmodified dataset to segregate MAMEs from the other confounding noises in the dRNA-Seq platform. In this proof-of-concept study, we have substituted the need for such a null data set and demonstrated that the acrylonitrile`s selective reactivity with A-I and Ψ modification induces a distinct profile to validate that MAME from noise. The nanoRMS workflow shows that chemical probes efficiently alter trace value along with signal intensity (**Figure 4H**). Since acrylonitrile has the optimal reactivity towards I-modification[12], we employed it in this proof-of-concept study to demonstrate the adaptation of a chemical probe in the dRNA-Seq platform for revealing actual I modification. Future studies will focus on screening the new chemical probes, specifically, the derivatives of acrylonitrile of varying sizes[31];[32] and physicochemical properties with attentive consideration of its impact on ONT parameters.

Our dRNA-Seq on mouse brain revealed bonafide A-I sites through mismatch errors. However, the unbiased denovo capturing of A-I modifications using chemical probe-induced signal difference was hindered by lower coverage. Nevertheless, we addressed the issue of low coverage associated with the dRNA-Seq by developing Nano ICE-Seq, which efficiently captures A-I sites that were not sampled by dRNA-Seq. A-I differential editing is implicated in psychiatric disorders such as autism, schizophrenia, and epilepsy[9]. The `Quick to Adapt` Nano ICE-Seq with 30 h runtime (experiment to analysis) could be efficiently utilized to probe clinically relevant differential A-I sites as diagnostic or prognostic markers.

Supporting Information

All the materials and methods including the new workflow called Nano ICE-Seq are detailed in the supporting information. The description of the extraction of nanopore parameters, support vector machine learning and TOMBO analysis are also given along with the supplementary figures and tables.

Author Contributions

S.R and V.J.S. contributed equally to this work. S.R. conceived the idea. G.N.P, S.R and V.J.S. designed the work. S.R and V.J.S. performed research, S.S assisted in the dRNA-Seq run. S.R. analyzed the data. L.C., T.H., Y.Z. and H.S. gave critical comments to improve the work. V.T. assisted with characterization studies. S.R. wrote the manuscript. G.N.P. editing and review of final draft. The authors declare no conflict of interest.

Data Availability

All FASTQ files generated in this work are submitted at European Nucleotide Archive (ENA) and will be made publicly available.

Funding Sources

This work was supported by Japan Society for the Promotion of Science (JSPS) KAKENHI [Grant No. JP19H03349; 22K19291] and Uehara Memorial Foundation to G.N.P. We thank JSPS [Grant No. 21H04705 and 20H05936] and AMED [Grant No. JP18am0301005] and, [JP20am0101101] and NIHR01 CA236350 to H.S. We thank MEXT fellowship for V.J.S. We also thank JSPS [S19127]; NIH/NEI [EY031439-01]; NJCSCR grant [151RG006] and Rutgers - TechAdvance Fund.

References

(1) Boccaletto, P.; Machnicka, M. A.; Purta, E.; Piątkowski, P.; Bagiński, B.; Wirecki, T. K.; de Crécy-Lagard, V.; Ross, R.; Limbach, P. A.; Kotter, A.; Helm, M.; Bujnicki, J. M. MODOMICS: A Database of RNA Modification Pathways.

2017 Update. *Nucleic Acids Research*. 2018, pp D303–D307. https://doi.org/10.1093/nar/gkx1030.
(2) Seelam, P. P.; Sharma, P.; Mitra, A. Structural Landscape of Base Pairs Containing Post-Transcriptional Modifications in RNA. *RNA* **2017**, *23* (6), 847–859.
(3) Behm, M.; Öhman, M. RNA Editing: A Contributor to Neuronal Dynamics in the Mammalian Brain. *Trends Genet.* **2016**, *32* (3), 165–175.
(4) Licht, K.; Hartl, M.; Amman, F.; Anrather, D.; Janisiw, M. P.; Jantsch, M. F. Inosine Induces Context-Dependent Recoding and Translational Stalling. *Nucleic Acids Res.* **2019**, *47* (1), 3–14.
(5) Brümmer, A.; Yang, Y.; Chan, T. W.; Xiao, X. Structure-Mediated Modulation of mRNA Abundance by A-to-I Editing. *Nat. Commun.* **2017**, *8* (1), 1255.
(6) Karikó, K.; Muramatsu, H.; Welsh, F. A.; Ludwig, J.; Kato, H.; Akira, S.; Weissman, D. Incorporation of Pseudouridine into mRNA Yields Superior Nonimmunogenic Vector with Increased Translational Capacity and Biological Stability. *Mol. Ther.* **2008**, *16* (11), 1833–1840.
(7) Yoon, K.-J.; Ringeling, F. R.; Vissers, C.; Jacob, F.; Pokrass, M.; Jimenez-Cyrus, D.; Su, Y.; Kim, N.-S.; Zhu, Y.; Zheng, L.; Kim, S.; Wang, X.; Doré, L. C.; Jin, P.; Regot, S.; Zhuang, X.; Canzar, S.; He, C.; Ming, G.-L.; Song, H. Temporal Control of Mammalian Cortical Neurogenesis by mA Methylation. *Cell* **2017**, *171* (4), 877–889.e17.
(8) García-López, J.; Hourcade, J. de D.; Del Mazo, J. Reprogramming of microRNAs by Adenosine-to-Inosine Editing and the Selective Elimination of Edited microRNA Precursors in Mouse Oocytes and Preimplantation Embryos. *Nucleic Acids Res.* **2013**, *41* (10), 5483–5493.
(9) Slotkin, W.; Nishikura, K. Adenosine-to-Inosine RNA Editing, and Human Disease. *Genome Medicine*. 2013, p 105. https://doi.org/10.1186/gm508.
(10) Burns, C. M.; Chu, H.; Rueter, S. M.; Hutchinson, L. K.; Canton, H.; Sanders-Bush, E.; Emerson, R. B. Regulation of Serotonin-2C Receptor G-Protein Coupling by RNA Editing. *Nature* **1997**, *387* (6630), 303–308.
(11) Nishimoto, Y.; Yamashita, T.; Hideyama, T.; Tsuji, S.; Suzuki, N.; Kwak, S. Determination of Editors at the Novel A-to-I Editing Positions. *Neurosci. Res.* **2008**, *61* (2), 201–206.
(12) Sakurai, M.; Yano, T.; Kawabata, H.; Ueda, H.; Suzuki, T. Inosine Cyanoethylation Identifies A-to-I RNA Editing Sites in the Human Transcriptome. *Nat. Chem. Biol.* **2010**, *6* (10), 733–740.
(13) Khoddami, V.; Yerra, A.; Mosbruger, T. L.; Fleming, A. M.; Burrows, C. J.; Cairns, B. R. Transcriptome-Wide Profiling of Multiple RNA Modifications Simultaneously at Single-Base Resolution. *Proc. Natl. Acad. Sci. U. S. A.* **2019**, *116* (14), 6784–6789.
(14) Kasianowicz, J. J.; Brandin, E.; Branton, D.; Deamer, D. W. Characterization of Individual Polynucleotide Molecules Using a Membrane Channel. *Proc. Natl. Acad. Sci. U. S. A.* **1996**, *93* (24), 13770–13773.
(15) Howorka, S.; Cheley, S.; Bayley, H. Sequence-Specific Detection of Individual DNA Strands Using Engineered Nanopores. *Nat. Biotechnol.* **2001**, *19* (7), 636–639.
(16) Garalde, D. R.; Snell, E. A.; Jachimowicz, D.; Sipos, B.; Lloyd, J. H.; Bruce, M.; Pantic, N.; Admassu, T.; James, P.; Warland, A.; Jordan, M.; Ciccone, J.; Serra, S.; Keenan, J.; Martin, S.; McNeill, L.; Jayne Wallace, E.; Jayasinghe, L.; Wright, C.; Blasco, J.; Young, S.; Brocklebank, D.; Juul, S.; Clarke, J.; Heron, A. J.; Turner, D. J. Highly Parallel Direct RNA Sequencing on an Array of Nanopores. *Nature Methods*. 2018, pp 201–206. https://doi.org/10.1038/nmeth.4577.
(17) Smith, A. M.; Jain, M.; Mulroney, L.; Garalde, D. R.; Akeson, M. Reading Canonical and Modified Nucleobases in 16S Ribosomal RNA Using Nanopore Native RNA Sequencing. *PLoS One* **2019**, *14* (5), e0216709.
(18) Jenjaroenpun, P.; Wongsurawat, T.; Wadley, T. D.; Wassenaar, T. M.; Liu, J.; Dai, Q.; Wanchai, V.; Akel, N. S.; Jamshidi-Parsian, A.; Franco, A. T.; Boysen, G.; Jennings, M. L.; Ussery, D. W.; He, C.; Nookaew, I. Decoding the Epitranscriptional Landscape from Native RNA Sequences. *Nucleic Acids Res.* **2021**, *49* (2), e7.
(19) Fleming, A. M.; Mathewson, N. J.; Howpay Manage, S. A.; Burrows, C. J. Nanopore Dwell Time Analysis Permits Sequencing and Conformational Assignment of Pseudouridine in SARS-CoV-2. *ACS Cent Sci* **2021**, *7* (10), 1707–1717.
(20) Huang, S.; Zhang, W.; Katanski, C. D.; Dersh, D.; Dai, Q.; Lolans, K.; Yewdell, J.; Eren, A. M.; Pan, T. Interferon Inducible Pseudouridine Modification in Human mRNA by Quantitative Nanopore Profiling. *Genome Biol.* **2021**, *22* (1), 330.
(21) Liu, H.; Begik, O.; Lucas, M. C.; Ramirez, J. M.; Mason, C. E.; Wiener, D.; Schwartz, S.; Mattick, J. S.; Smith, M. A.; Novoa, E. M. Accurate Detection of mA RNA Modifications in Native RNA Sequences. *Nat. Commun.* **2019**, *10* (1), 4079.
(22) Stoiber, M.; Quick, J.; Egan, R.; Lee, J. E.; Celniker, S.; Neely, R. K.; Loman, N.; Pennacchio, L. A.; Brown, J. De novoIdentification of DNA Modifications Enabled by Genome-Guided Nanopore Signal Processing. https://doi.org/10.1101/094672.
(23) Yoshida, M.; Ukita, T. Modification of Nucleosides and Nucleotides. VII. Selective Cyanoethylation of Inosine and Pseudouridine in Yeast Transfer Ribonucleic Acid. *Biochim. Biophys. Acta* **1968**, *157* (3), 455–465.
(24) Lo Giudice, C.; Silvestris, D. A.; Roth, S. H.; Eisenberg, E.; Pesole, G.; Gallo, A.; Picardi, E. Quantifying RNA Editing in Deep Transcriptome Datasets. *Front. Genet.* **2020**, *11*, 194.
(25) Sakurai, M.; Suzuki, T. Biochemical Identification of A-to-I RNA Editing Sites by the Inosine Chemical Erasing (ICE) Method. *Methods Mol. Biol.* **2011**, *718*, 89–99.
(26) Begik, O.; Lucas, M. C.; Pryszcz, L. P.; Ramirez, J. M.; Medina, R.; Milenkovic, I.; Cruciani, S.; Liu, H.; Vieira, H. G. S.; Sas-Chen, A.; Mattick, J. S.; Schwartz, S.; Novoa, E. M. Quantitative Profiling of Pseudouridylation Dynamics in Native RNAs with Nanopore Sequencing. *Nat. Biotechnol.* **2021**. https://doi.org/10.1038/s41587-021-00915-6.
(27) Mengel-Jørgensen, J.; Kirpekar, F. Detection of Pseudouridine and Other Modifications in tRNA by Cyanoethylation and MALDI Mass Spectrometry. *Nucleic Acids Res.* **2002**, *30* (23), e135.
(28) Ramaswami, G.; Li, J. B. RADAR: A Rigorously Annotated Database of A-to-I RNA Editing. *Nucleic Acids Res.* **2014**, *42* (Database issue), D109–D113.
(29) Picardi, E.; D'Erchia, A. M.; Lo Giudice, C.; Pesole, G. REDIportal: A Comprehensive Database of A-to-I RNA Editing Events in Humans. *Nucleic Acids Res.* **2017**, *45* (D1), D750–D757.
(30) Li, X.; Zhu, P.; Ma, S.; Song, J.; Bai, J.; Sun, F.; Yi, C. Chemical Pulldown Reveals Dynamic Pseudouridylation of the Mammalian Transcriptome. *Nat. Chem. Biol.* **2015**, *11* (8), 592–597.
(31) Knutson, S. D.; Korn, M. M.; Johnson, R. P.; Monteleone, L. R.; Dailey, D. M.; Swenson, C. S.; Beal, P. A.; Heemstra, J. M. Chemical Profiling of A-to-I RNA Editing Using a Click-Compatible Phenylacrylamide. *Chemistry* **2020**, *26* (44), 9874–9878.
(32) Knutson, S. D.; Ayele, T. M.; Heemstra, J. M. Chemical Labeling and Affinity Capture of Inosine-Containing RNAs Using Acrylamidofluorescein. *Bioconjug. Chem.* **2018**, *29* (9), 2899–2903.

Graphical Abstract